Received: 21 January 2022 | Revised: 18 April 2022 | Accepted: 22 April 2022

DOI: 10.1096/fj.202200120R

THE FASEB JOURNAL

RESEARCH ARTICLE

Pericyte dynamics in the mouse germinal matrix angiogenesis

Taliha Nadeem | **Apoorva Bommareddy** | **Lolade Bolarinwa** | **Henar Cuervo**

Department of Physiology and Biophysics, College of Medicine, University of Illinois at Chicago, Chicago, Illinois, USA

Correspondence
Henar Cuervo, Department of Physiology and Biophysics, College of Medicine, University of Illinois at Chicago, 835 S. Wolcott Avenue E-202, Chicago, IL 60612, USA.
Email: hcuervo@uic.edu

Funding information
University of Illinois Chicago; UIC Provost's Award for Graduate Research

Abstract

Germinal matrix-intraventricular hemorrhage (GM-IVH) is the most devastating neurological complication in premature infants. GM-IVH usually begins in the GM, a highly vascularized region of the developing brain where glial and neuronal precursors reside underneath the lateral ventricular ependyma. Previous studies using human fetal tissue have suggested increased angiogenesis and paucity of pericytes as key factors contributing to GM-IVH pathogenesis. Yet, despite its relevance, the mechanisms underlying the GM vasculature's susceptibility to hemorrhage remain poorly understood. To gain better understanding on the vascular dynamics of the GM, we performed a comprehensive analysis of the mouse GM vascular endothelium and pericytes during development. We hypothesize that vascular development of the mouse GM will provide a good model for studies of human GM vascularization and provide insights into the role of pericytes in GM-IVH pathogenesis. Our findings show that the mouse GM presents significantly greater vascular area and vascular branching compared to the developing cortex (CTX). Analysis of pericyte coverage showed abundance in PDGFRβ-positive and NG2-positive pericyte coverage in the GM similar to the developing CTX. However, we found a paucity in Desmin-positive pericyte coverage of the GM vasculature. Our results underscore the highly angiogenic nature of the GM and reveal that pericytes in the developing mouse GM exhibit distinct phenotypical and likely functional characteristics compared to other brain regions which might contribute to the high susceptibility of the GM vasculature to hemorrhage.

KEYWORDS
angiogenesis, germinal matrix, intraventricular hemorrhage, mice, pericytes

Abbreviations: ANGPT, angiopoietin; CTX, cortex; E, embryonic day; GA, gestational age in weeks; GFAP, glial fibrillary acidic protein; GM, germinal matrix; GM-IVH, germinal matrix-intraventricular hemorrhage; IB4, Isolectin B4; LV, lateral ventricle; N-cadherin, neural cadherin; NG2, neuron-glial antigen-2; NPC, neural progenitor cell; NVU, neurovascular unit; P, postnatal day; PDGF-B, platelet-derived growth factor-B; PDGFRβ, platelet-derived growth factor receptor beta; S1P, sphingosine-1-phosphate; SVZ, subventricular zone; TGF-β1, transforming growth factor-beta 1; VEGF-A, vascular endothelial growth factor-A; αSMA, alpha-smooth muscle actin.

1 | INTRODUCTION

Germinal matrix-intraventricular hemorrhage (GM-IVH) is a highly feared complication in premature infants affecting approximately 12 000 newborns every year in the United States.[1] The GM is a highly vascularized region of the developing brain where glial and neuronal precursors reside underneath the lateral ventricular ependyma[1]; it reaches its maximum volume around 25 weeks of gestational age, and progressively involutes into a residual mass present at 36 weeks of gestational age.[2,3] When severe GM hemorrhage occurs, the ventricular ependyma breaks filling the ventricles with blood and resulting in IVH.[1] GM-IVH survivors often develop neurodevelopmental impairments and, to a lesser extent, cerebral palsy, cognitive defects, and intellectual disabilities.[4–7] Treatment to date is focused on glucocorticoid administration antenatally, which provides improved disease outcome, but there is an obvious unmet need for better therapeutics.[8]

Why hemorrhage in the premature infant brain occurs preferentially in the GM is not known, since the pathogenesis of GM-IVH is complex and multifactorial, but is usually attributed to the intrinsic fragility of the GM capillaries, disturbances in cerebral blood flow, and some genetic factors.[1] The vasculature of the GM displays differential characteristics compared to that of the developing cerebral cortex (CTX) or white matter; one of these key differences is the high vascularity of the GM observed during human fetal development.[9] Previous literature characterizes the vasculature of the GM as an immature network that is remodeled into a mature capillary bed as the GM involutes.[10] In the human fetal brain, the percentage of vessel area and the number of blood vessels have been found to be greater in the GM for all gestational ages when compared to other regions of the brain.[9] This high vascularity is attributed to the presence of a highly angiogenic microenvironment.[11] In the human GM, vascular endothelial growth factor-A (VEGF-A), the predominant angiogenic growth factor during vascular development,[12] was highest in contrast to other brain regions.[11] These findings have led to the current model which proposes that the increased exposure of the fetal GM vasculature to angiogenic factors promoting angiogenesis would prevent the blood vessels from maturing resulting in an immature vascular network with increased fragility compared with vessels of other brain regions.

Another distinctive feature of the GM vasculature observed during fetal development is the paucity of pericytes.[13] Pericytes are perivascular cells of the capillaries.[14] They have essential functions during cerebrovascular development and maturation.[14–17] During angiogenesis, pericyte recruitment to the newly developed blood vessels is mediated by the release of platelet-derived growth factor-B (PDGF-B) by angiogenic endothelial cells.[18] PDGF-B binds to the corresponding receptor, platelet-derived growth factor receptor beta (PDGFRβ), which is expressed by pericytes.[19] PDGFRβ-positive pericytes are then recruited to the nascent blood vessels and stabilize the growing vasculature by arresting endothelial cell proliferation and by synthesizing components of the basement membrane.[20,21] Not surprisingly, the loss and/or dysfunction of pericytes results in abnormal angiogenesis and hemorrhage.[14,22]

In the GM, PDGFRβ-positive pericyte coverage has been evaluated in fetal samples and found significantly reduced compared to other regions of the developing brain.[13] This paucity of pericytes is consistent with the reported increased vascularity and angiogenic nature described for the GM and underscores the concept that the vasculature of the GM shows features of immaturity compared to other brain regions.[13]

Thus far, the majority of our understanding of the GM vasculature comes from studies using human fetal or premature infant samples that appeared healthy but were nonviable.[9,11,13] These important studies, however, are limited by factors related to the use of post-mortem human tissue including sample availability, accessibility, and quality. Appropriate animal models are an invaluable tool to overcome some of these technical limitations and better dissect the causative factors and the pathogenesis of GM-IVH. Mice in particular, are easily accessible for genetic manipulations making them ideal animal models to study different human diseases and disease processes. Several investigators have used mouse models to begin addressing the cellular basis of intracerebral hemorrhage in mice.[23–29] However, the developmental anatomy and vascularization of the GM in mice have not been well documented. Thus, it is unclear how phenotypically comparable the developmental mouse GM is to that of the developmental human GM limiting the confidence of the use of mouse models to uncover the bases of GM-IVH pathogenesis and in preclinical studies. We hypothesize that vascular development of the mouse GM will provide a good model for studies of human GM vascularization and provide insights into the role of pericytes in GM-IVH pathogenesis.

In this study, we provide a comprehensive analysis of the mouse GM vasculature during development. Our findings show that similar to the human GM, the mouse GM also undergoes stages of growth and involution and is highly vascularized compared to other brain regions. Unexpectedly, pericyte coverage in the mouse GM is highly abundant as opposed to the paucity of pericytes described in the human GM. We also found that the mouse GM is heterogenous in its expression of pericyte markers, which may influence the GM susceptibility to hemorrhage. Our findings highlight important similarities and differences

between the human and the mouse GM which should be considered towards the use of mice to model or study the pathogenesis of GM-IVH.

2 | MATERIAL AND METHODS

2.1 | Mice

Wild-type (C57BL/6J, JAX: 000664) mice from embryonic (E) 10.5 to postnatal (P) 5 days old were used for our studies for the evaluation of GM and CTX growth, vascularization and pericyte coverage.

PDGFRβ-P2A-CreER^{T2}[30] were interbred with *Rosa26*$^{\text{tdTomato}}$ (*Gt(ROSA)26Sor*$^{tm9(CAG-tdTomato)Hze}$, JAX: 007909) mice[31] in order to monitor recombination efficiency and specificity, and for further data acquisition. *PDGFRβ-P2A-CreER*^{T2} were also interbred with *Rosa26*$^{\text{mTmG}}$ (Gt(ROSA)26Sor$^{\text{tm4(ACTB-tdTomato,-EGFP)Luo}}$, JAX: 007676) mice[32] to evaluate pericyte morphology.

For Cre-mediated recombination, pregnant females were treated with 3 mg/day of tamoxifen (Sigma, T5648; dissolved in corn oil (Sigma, C8267) at 30 mg/ml) by oral gavage on E10.5 and E11.5.

All experiments were performed in compliance with the Animal Care Committee guidelines at the University of Illinois at Chicago under protocol ACC 22-014. Animals were maintained and treated with humane care according to the *Guide for the Care and Use of Laboratory Animals*.[33] Females and males were used indistinctively in these studies.

All data were analyzed and reported in compliance with the ARRIVE (Animal Research: Reporting In Vivo Experiments) guidelines.

2.2 | Tissue collection and sample processing

Plugged females were euthanized at the appropriate embryonic age (E10.5, E11.5, E14.5, E16.5, or E18.5) by CO_2 asphyxiation and cervical dislocation. Embryos were harvested and processed as previously described.[29] Briefly, after removing the yolk sac and the embryonic membranes, whole embryos were collected at E10.5, E11.5, and E14.5 time points, and brains were collected at E16.5 and E18.5. For postnatal studies, mice were decapitated, and brains were collected at P5.

Collected tissues were fixed in 4% formaldehyde (Thermo Fisher Scientific) overnight at 4°C. After fixation, tissues were cryoprotected by immersion in 30% sucrose solution in PBS for 24 h at 4°C, embedded into OCT (Tissue Tek) and stored at −80°C until sectioning.

2.3 | Immunofluorescence staining

Forebrain coronal sections (40 μm) were incubated with permeabilizing solution in 1× PBS containing 1% BSA (Fisher Bioreagents) and 0.5% Triton-X-100 (Fisher Bioreagents) overnight at 4°C on a nutator. Samples were then immunostained in PBLEC (5% Triton X-100, 1 M $MgCl_2$, 1 M $CaCl_2$, and 1 M $MnCl_2$ in 1X PBS) overnight at 4°C with Biotinylated IB4 (1:50; Vector Laboratories; Cat# BAF1042) and/or the following antibodies: goat anti-PDGFRβ (1:100; R&D Systems; Cat# BAF1042), rabbit anti-NG2 (1:700; Millipore; Cat# AB5320), rabbit anti-Desmin (1:500; Abcam; Cat# AB15200), anti–αSMA-FITC (1:200; Millipore Sigma, Cat# F3777). Following primary antibodies, sections were incubated in the secondary antibodies overnight at 4°C. Secondary antibodies used were Streptavidin Alexa 647, and Alexa 488-, 594-conjugated donkey anti-rabbit or anti-goat (1:700; Invitrogen). After completion of staining, slides were mounted using antifade mounting medium with DAPI (Vector Laboratories).

2.4 | Image acquisition and data analysis

Confocal imaging (20×, 40× with water immersion or 63× with oil immersion) was performed on a Zeiss LSM 880 Confocal microscope with Airyscan (Carl Zeiss). Image J software (National Institute of Health) was used for quantification and analysis of the GM and the CTX.

Vessel area was quantified as the threshold value of IB4-positive endothelial cells per total field area (mm^2). The number of IB4-positive vessel branches was quantified per field area (mm^2). For vessel diameter, 10 measurements of vessel width per field were acquired and the average diameter was calculated and plotted. For PDGFRβ-positive pericyte coverage, PDGFRβ and IB4 staining overlap was calculated as previously described.[34] Similarly, NG2 and IB4 staining overlap was calculated for NG2-positive pericyte coverage. Desmin-positive pericyte coverage was calculated as a percentage of Desmin staining threshold value over vascular staining threshold value.

To quantify the number of pericytes in the GM and the CTX, we defined pericytes ($NG2^+$; $PDGFR\beta^-$, $PDGFR\beta^+$; $NG2^-$, $PDGFR\beta^+$; $NG2^+$, $Desmin^+$; $PDGFR\beta^-$, $PDGFR\beta^+$; $Desmin^-$, $PDGFR\beta^+$; $Desmin^+$) as cells with a distinct, round protruding cell body with processes in close proximity to the IB4-positive blood vessels, as described previously.[35]

tdTomato recombination in pericytes was measured as the percentage of tdTomato reporter expression associated with $NG2^+$ pericytes.

To document GM and CTX growth and involution, tiled images (8×) were acquired on Zeiss Axio Zoom.V16 (Carl Zeiss). Using DAPI staining, ten measurements of the GM and CTX width were made within the same section; the average width was calculated and plotted.

2.5 | Statistical methods

All data were plotted and analyzed using GraphPad Prism 9. In the study, n refers to the number of animals used per timepoint evaluated. Since this was an exploratory experiment, we did not formally perform a priori power analyses. Data were checked for normality using the Shapiro-Wilk test and were analyzed using a two-way ANOVA with Bonferroni's multiple comparisons test. For non-normal variables, the Mann-Whitney *U* test was applied. $p < .05$ was considered to be statistically different. Data are presented as mean ± SD.

3 | RESULTS

3.1 | Timeline of germinal matrix growth and involution in mice

The germinal matrix (GM) is a highly vascularized area of the developing brain. It is located adjacent to the wall of the lateral ventricles (LVs), comprising of the lateral and medial ganglionic eminences in the ventral telencephalon region of the developing forebrain.[36] In the human brain, the GM growth and involution has been thoroughly studied: the GM is first observed at 7–9 weeks of gestational age, it is greatest between 20 and 26 weeks, and it is almost completely involuted by 33 weeks.[2,3,37] However, at present, a thorough assessment of the developmental events of the mouse GM has not been reported.

To provide a comprehensive timeline of the growth and involution of the GM in mice, we collected forebrains from C57BL/6J wild-type mice at different time points of development, beginning at embryonic day (E) 10.5 when previous studies report the medial ganglionic eminences are first observed.[38,39] We stained cryosections using DAPI to identify the GM as the region of the brain located adjacent to the ventral wall of the LVs consisting of small, round, and densely packed cells as previously described.[3] GM width was quantified in parallel with the developing CTX at several time points: E10.5, E11.5, E14.5, E16.5, E18.5, and postnatal (P) day 5 (Figure 1A–D). We observed GM expansion in width from E10.5 (~100 μm) until E14.5, when it was widest (>500 μm) (Figure 1B,D). After E14.5 the GM width decreased and by postnatal day (P) 5, the GM had involuted to a small region (<50 μm) referred to as the postnatal subventricular zone (SVZ) (Figure 1B,D).[39] As a reference, the development the CTX, continued expanding exponentially in size from E10.5 to P5 (Figure 1A,C). Overall these findings provide a comprehensive assessment of

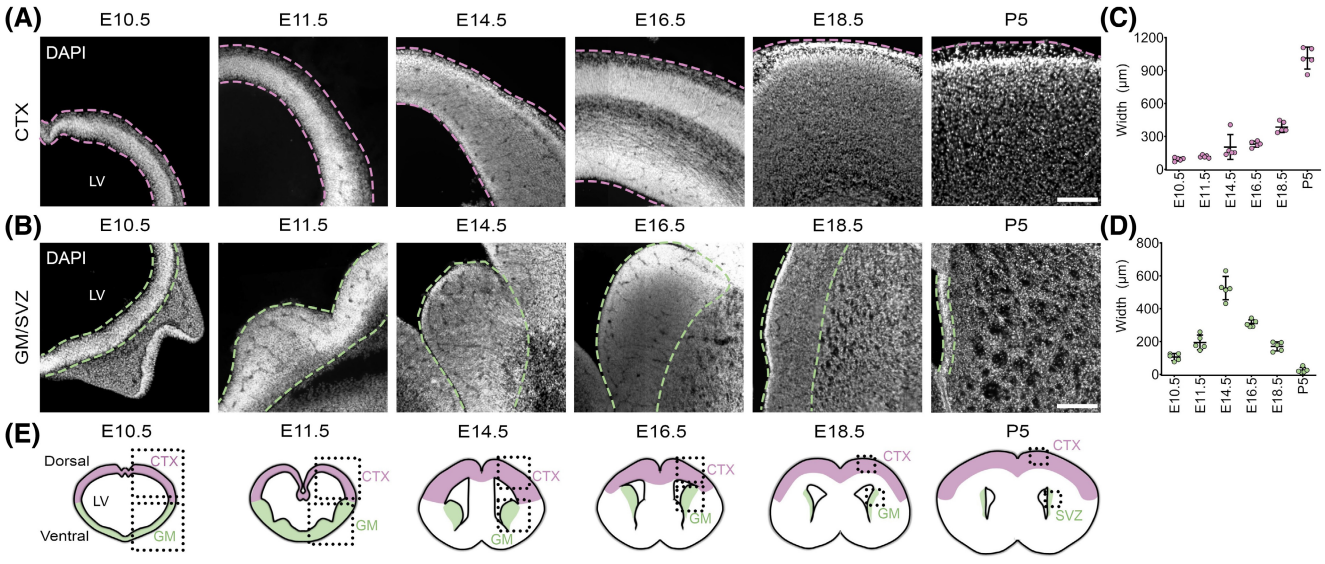

FIGURE 1 The GM of mice grows in size until E14.5 and involutes by P5. (A,B) Coronal sections stained with DAPI (white) to identify the developing cerebral cortex (CTX), germinal matrix (GM) and postnatal subventricular zone (SVZ) regions. Dashed lines highlight the CTX (purple) and GM/SVZ[63] regions of the brain. (C,D) Quantification of CTX (C) and GM (D) width during development. Scatter dot plots show mean values with standard deviation. $n = 5$ mice for all time points. (E) Scheme of the developing CTX and GM during development E10.5–P5. Dashed boxes represent fields used in measuring the CTX and GM width. LV, lateral ventricles; E, embryonic; P, postnatal. Scale bar, 190 μm

the developmental stages of GM growth and involution in the mouse embryo (Figure 1E).

3.2 | The mouse GM exhibits increased vascularity compared to the developing CTX

Premature infants affected by GM-IVH primarily bleed in the GM and not in other regions of the brain, such as the developing cerebral CTX, suggesting there is an intrinsic fragility of the blood vessels of the GM compared with vessels of other brain regions.[1] This prompted us to examine the vasculature of the GM in mice during development and aim to identify differences in the GM vasculature compared to the developing CTX.

To evaluate the vasculature of the GM and the CTX, we immunostained cryosections of wild-type mouse forebrains at different time points, from E10.5 to P5, using Isolectin B4 (IB4) to label the blood vessels (Figure 2A,B). Consistent with previous findings,[27,29] we observed that vascularization of the GM begins at E10.5 when the vessels first sprout from the outer pia-associated vascular plexus towards the LV (Figure 2B). At E11.5, the vessels begin expanding dorsally into the developing CTX (Figure 2A).[29,40] We evaluated vessel area in the GM and the CTX over time until P5. We observed a steady increase in vessel area in the GM from E10.5 until E18.5 (Figure 2C). When compared to the CTX, where vessel area increased until E14.5, the GM had significantly greater vessel area at most of the timepoints analyzed (Figure 2A–C). To determine if the increased vessel area was due to an increase in the number of blood vessels or an increase in blood vessel size, we evaluated the number of vessel branches over time. Analysis of the number of vessel branches in the GM and the CTX showed an increase akin to that of the vessel area. The number of vessel branches was also significantly greater in the GM than the CTX (Figure 2D). We next measured the vessel diameter at the different time points. All of the time points analyzed showed no significant differences between the GM and the CTX (Figure 2E). Taken together, our data indicate that the mouse GM exhibits increased vascularity compared to the CTX due to an increased number of vessel branches, and not due to increased vessel diameter.

3.3 | Similar pericyte coverage between the GM and the developing CTX in mice

Pericytes have well-described roles in cerebrovascular development and maturation.[14–17] Previous literature has shown that there is a paucity of pericytes in the GM of healthy-appearing, nonviable premature infants,[13] suggesting that this feature of the GM vasculature is a key contributor to rendering it susceptible to hemorrhage upon premature birth. To gain further insights into the dynamics of pericytes in mouse GM, we evaluated the pericyte coverage of the GM and the CTX at different time points during development. For this purpose, we performed immunofluorescent staining of pericytes and the endothelium. We used IB4 to label the endothelium, and anti-PDGFRβ to label pericytes. We selected PDGFRβ as a primary marker for studying pericytes since it has been reported to be expressed consistently across all stages of brain development.[35] We analyzed pericyte coverage of the GM and CTX vessels at different time points (E10.5–P5) as shown in Figure 3(C). Consistent with previous literature,[27,41] we observed very few PDGFRβ-positive pericytes in the GM at E10.5 (Figure 3B,D). There was a further increase in their recruitment to the GM and CTX vasculatures from E11.5 onwards (Figure 3A,B,D). We also observed an increase in pericyte coverage during development in both regions of the brain. Surprisingly, we did not observe any significant differences between the PDGFRβ-positive pericyte coverage of the vessels in the GM and the CTX at any developmental time point evaluated (Figure 3D). In fact, pericytes appeared similarly associated with the endothelium in both the GM and the CTX (Figure 3A,B), in contrast to previous studies in humans, which reported a paucity in pericyte coverage using PDGFRβ.[13] In conclusion, our findings point to a similar pericyte coverage between the GM and the CTX vasculature during mouse embryonic brain development highlighting an important difference between the human and the mouse GMs.

3.4 | Delayed pericyte acquisition of NG2 expression in the GM

The absence of any differences in PDGFRβ-positive pericyte coverage in either the GM or the CTX prompted us to evaluate other pericyte markers in the developing GM. Currently, the known pericyte markers expressed during embryonic mouse brain development are PDGFRβ, neuron-glial antigen-2 (NG2) (both of which are membrane-expressed) and desmin, an intermediate filament.[35] To investigate potential differences in pericyte marker expression between the GM and CTX more thoroughly, we first immunostained embryonic mouse brain samples with IB4 to label the endothelium and performed dual labeling of pericytes using anti-PDGFRβ and anti-NG2 (Figure 4A,B). We observed that NG2-positive pericyte coverage was deficient in the GM at early stages

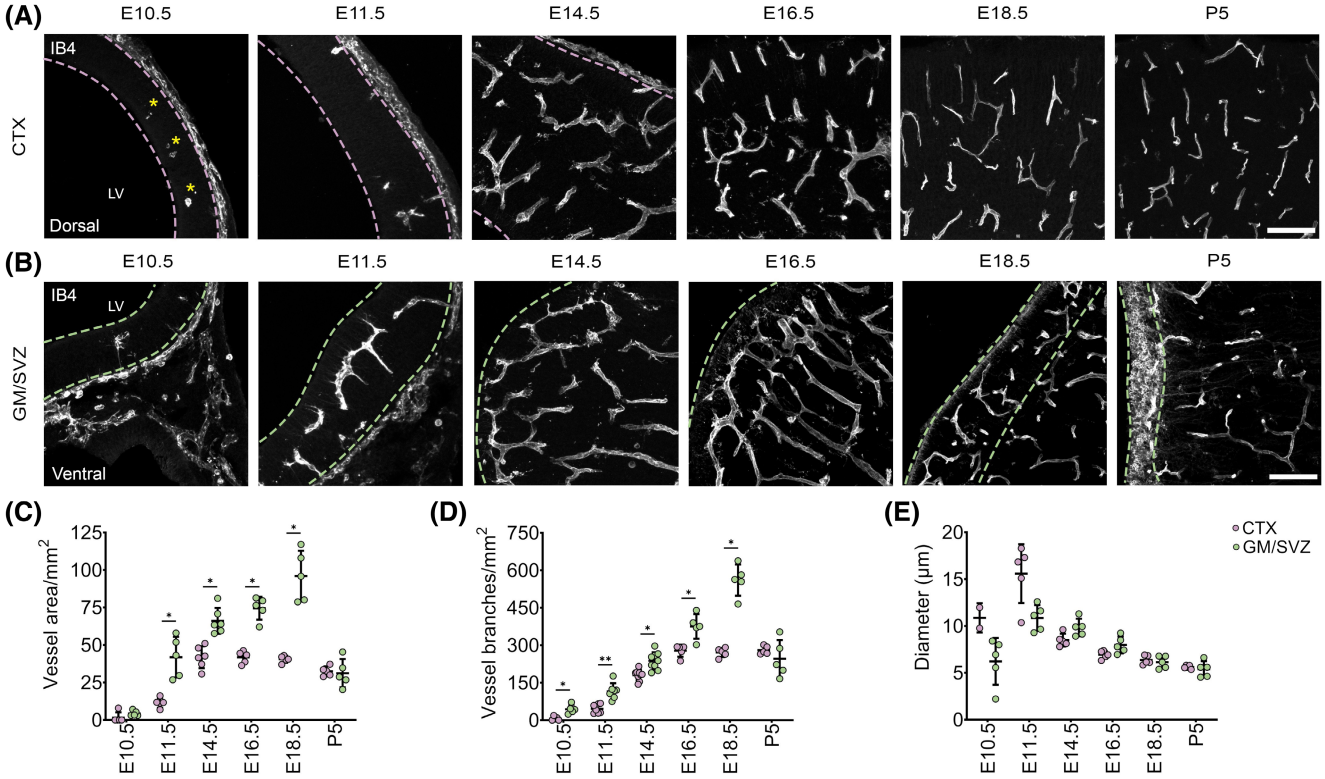

FIGURE 2 Greater vessel area and number of vessel branches in the mouse GM compared to the developing cerebral CTX. (A,B) Coronal sections stained with Isolectin B4 (IB4, white) to visualize the vasculature of the developing cortex (CTX, purple dashed lines) and the germinal matrix/postnatal subventricular zone (GM/SVZ, green dashed lines). Note that IB4 is also expressed by macrophages, which are present in the E10.5 CTX (yellow asterisk) and are excluded from the vessel analysis. (C–E) Quantification of vessel area (C), number of vessel branches (D), and vessel diameter (E) ($n = 5$–9). Scatter dot plots show mean values with standard deviation. Data was analyzed using a multiple comparison test using Mann-Whitney *U* test. *$p < .05$, **$p < .01$. LV, lateral ventricle; E, embryonic; P, postnatal. Scale bar, 100 μm

of vessel formation compared to the CTX (Figure 4A–C). From E11.5 onwards, there was an increase in NG2-positive pericyte coverage over development (E11.5–P5) in both the developing CTX and the GM. Further, there were no significant differences in coverage between the GM and the CTX from E14.5–P5, consistent with our results obtained using anti-PDGFRβ (Figure 4C).

To further evaluate the distribution of PDGFRβ-positive and NG2-positive pericytes between the different regions of the brain and over development, we quantified the number of pericytes in the GM and CTX expressing NG2 and PDGFRβ. We found that all NG2-positive pericytes expressed PDGFRβ. There was a small but notable population of PDGRβ$^+$; NG2$^-$ pericytes (11.97%) at E11.5 in the GM which was not present in the CTX (Figure 4D). From E14.5 onwards, there was an increase in the percentage of PDGRβ$^+$; NG2$^+$ pericytes (97%–100%) in the GM (Figure 4D). This data underscores the lack of significant differences in pericyte coverage previously observed between the GM and the CTX in humans. Additionally, it highlights a population of newly recruited PDGFRβ-positive pericytes that initially lack NG2 expression in the GM, suggesting pericytes of the GM may be more immature at early stages of angiogenesis compared to the CTX.

3.5 | The GM vasculature has a paucity of Desmin-positive pericyte coverage

We next immunostained the brain samples with IB4 to label the endothelium, and dual staining of pericytes using anti-PDGFRβ and anti-Desmin (Figure 5A,B). We evaluated Desmin-positive pericyte coverage of the endothelium during development (E11.5–P5). Our observation revealed that Desmin coverage increases in the CTX and the GM during development (Figure 5C). Interestingly, we observed that coverage was significantly lower in the GM compared to the developing CTX (Figure 5C). We next quantified the number of PDGFRβ-positive pericytes which express Desmin. While all Desmin-positive pericytes expressed PDGFRβ, we found some variability in the expression and distribution of PDGFRβ$^+$; Desmin$^+$ pericytes in the GM (64.47% at E11.5, 50.47% at E14.5, 43.49% at E16.5, 65.56% at E18.5, and 9.37% at P5) (Figure 5D).

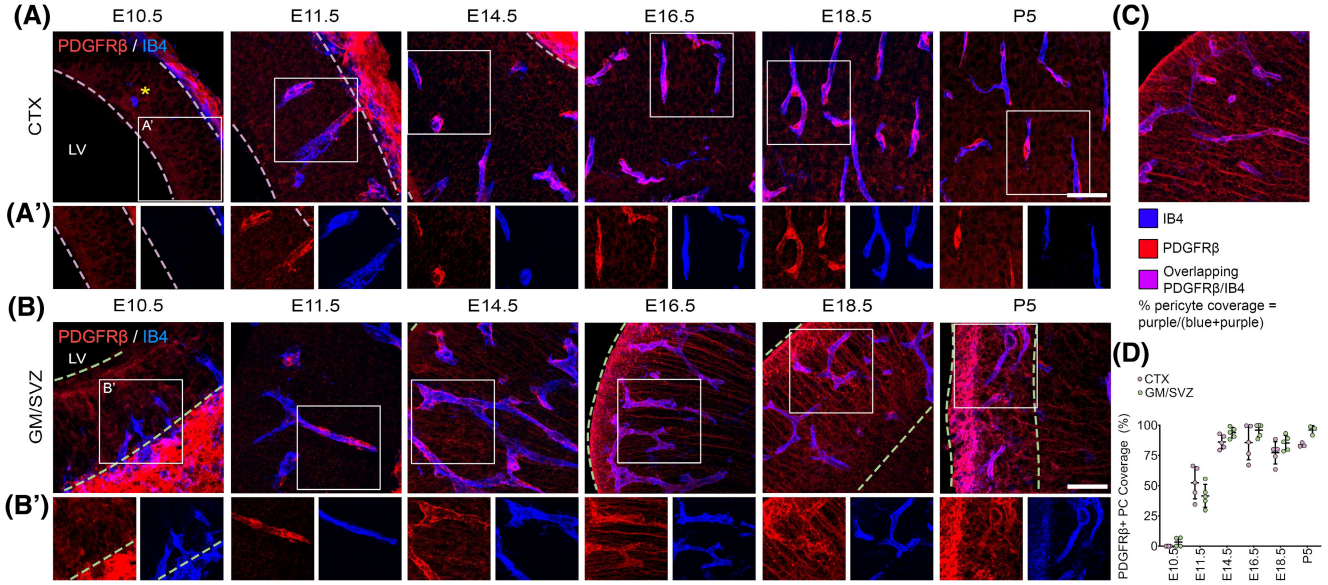

FIGURE 3 PDGFRβ-positive pericyte coverage is similar between the mouse GM and the developing cerebral CTX. (A,B) High magnification images of the developing cortex (CTX) and the germinal matrix/postnatal subventricular zone (GM/SVZ) stained for blood vessels using Isolectin B4 (IB4, blue), and for pericytes (anti-PDGFRβ, red). Purple dashed lines mark the CTX, and green dashed lines highlight the GM/SVZ regions. Yellow asterisk indicates IB4 labeled macrophages at E10.5 in the CTX. Cropped individual images (white solid boxes) of the endothelium and PDGFRβ-positive pericytes are displayed below each timepoint to best visualize pericyte coverage of the blood vessels (A′,B′). (C) Example of data and method used to quantify pericyte coverage (see Materials and Methods). (D) Quantification of pericyte coverage reveals no significant differences between the CTX and the GM. Scatter dot plot shows mean values with standard deviation $n = 5$ per time point except E10.5 ($n = 4$) and P5 ($n = 3$). Data was analyzed using a two-way ANOVA with Bonferroni's multiple comparison test. LV, lateral ventricles; E, embryonic; P, postnatal. Scale bar, 50 μm

Altogether, these observations suggest there is a deficiency of Desmin-positive pericytes in the GM.

Desmin is an intermediate filament associated with cell contractility.[42,43] Its deficient expression in pericytes of the GM prompted us to evaluate other markers associated with pericyte contractility. For this, we immunostained for anti-alpha-smooth muscle actin (αSMA), in addition to IB4 to label the endothelium. Our findings did not yield any αSMA expression in the GM or the CTX (Figure S1). This suggests to us pericytes of the developing mouse brain are not likely to exhibit major contractile functions.

3.6 | Pericytes of the mouse GM vasculature do not differ in morphology compared to the CTX

Pericyte identification relies heavily on specific marker expression and morphology. Our observations regarding the variability in marker expression of pericytes in the GM and CTX suggest the existence of different pericyte populations exhibiting distinct pericyte marker expression in the different brain regions. To further understand pericyte heterogeneity between the two brain regions, we evaluated pericyte morphology using *PDGFRβ-P2A-CreER*^{T2} mice to allow for Cre-mediated expression of tdTomato expression in pericyte nuclei using the *Rosa26*$^{\text{tdTomato}}$ reporter mice,[31] and also the expression of membrane localized EGFP using the *Rosa26*$^{\text{mTmG}}$ reporter mice.[32]

We have previously shown that the *PDGFRβ-P2A-CreER*^{T2} mouse line can efficiently target pericytes of the postnatal retina and brain.[30] To evaluate if pericytes of the embryonic mouse brain were also efficiently targeted, we induced tdTomato expression in *PDGFRβ-P2A-CreER*^{T2}; *Rosa26*$^{\text{tdTomato}}$ mice through tamoxifen administration to the pregnant female at E10.5 and E11.5, stages of initial vascularization of the brain. Recombination efficiency in pericytes at E14.5 in the GM and the CTX was 91.91 ± 1.42% and 95.34 ± 0.94% respectively (Figure S2A,B). We then evaluated the morphology of pericytes using tamoxifen treated *PDGFRβ-P2A-CreER*^{T2}; *Rosa26*$^{\text{tdTomato}}$ mice. Extensive analysis of the CTX and GM did not reveal any differences in pericyte morphology between these two brain regions (Figure S2C). For a more comprehensive analysis of the pericyte membrane morphology, we also evaluated pericytes using *PDGFRβ-P2ACreER*^{T2}; *Rosa26*$^{\text{mTmG}}$ mice. Analysis of these mice showed no obvious differences in pericyte morphology between the GM and CTX pericytes at E14.5 or E18.5 (Figure S2D).

Although out data suggests that pericyte morphology is comparable between the two brain regions, our observations

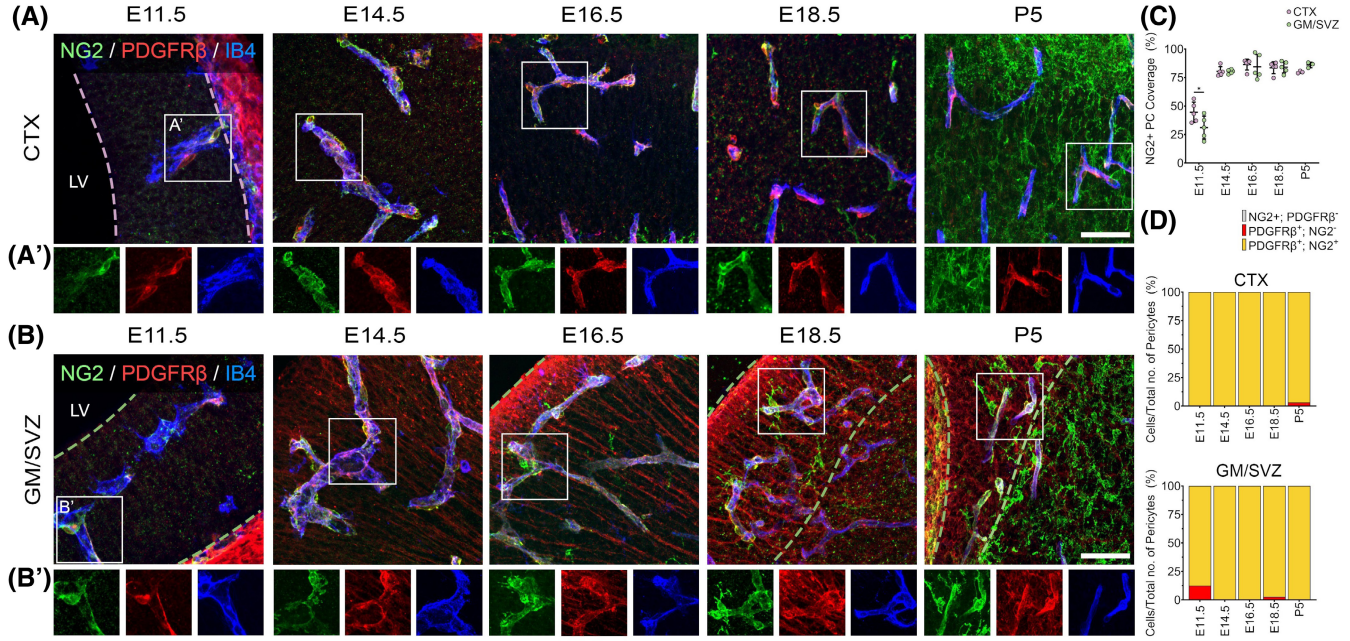

FIGURE 4 Delayed NG2 expression in pericytes of the mouse GM compared to the developing cerebral CTX. (A,B) High magnification images of the developing cortex (CTX) and the germinal matrix/postnatal subventricular zone (GM/SVZ) stained for blood vessels using Isolectin B4 (IB4, blue) and for pericytes with anti-PDGFRβ (red) and anti-NG2.[63] Purple dashed lines mark the CTX, and green dashed lines highlight the GM/SVZ regions. Cropped individual images (white solid boxes) of the endothelium and pericytes are displayed below each timepoint to best visualize the overlap of NG2 and PDGFRβ expression and pericyte coverage of the blood vessels (A′,B′). Note that in the CTX and the GM/SVZ, NG2 is also expressed by oligodendrocyte precursor cells beginning at E14.5; these cells were excluded from the analysis. (C) Quantification of NG2-positive pericyte coverage reveals reduced coverage at E11.5 in the GM. Scatter dot plot shows mean values with standard deviation. $n = 5$ per time point except P5 ($n = 3$). Data was analyzed using a two-way ANOVA with Bonferroni's multiple comparison test. $*p < .05$. (D) Quantification of $NG2^+$; $PDGFR\beta^-$ (gray), $PDGFR\beta^+$; $NG2^-$ (red) and $PDGFR\beta^+$; $NG2^+$ (yellow) pericytes over total pericytes counted per field. $n = 5$ per time point except P5 ($n = 3$). LV, lateral ventricles; E, embryonic; P, postnatal. Scale bar, 50 μm

regarding the heterogeneity in marker expression of pericytes in the GM and CTX point to the existence of different pericyte populations with distinct phenotypical and likely functional characteristics in the different brain regions. These differences may be an important contributor to the increased GM vasculature susceptibility to hemorrhage.

4 | DISCUSSION

Germinal matrix-intraventricular hemorrhage is a devastating complication affecting premature infants yet, despite its significance, the mechanisms underlying GM-IVH remain obscure. Much of our understanding of the GM vasculature comes from the autopsy brain samples from premature infants, which has led to propose a model where the intrinsic fragility of the GM vasculature, fluctuations in cerebral blood flow, and genetic factors together contribute to the pathogenesis of GM-IVH.[1] Increasingly over the past few years, a number of studies have begun using mice to interrogate the mechanisms of hemorrhage in the GM. These animal models include (1) lesion-induced models using glycerol,[44] blood and blood derivatives[45] and collagenase[46]; and (2) genetically modified models such as transgenic mice with mutations in the alpha-v subunit of integrins,[47] mice overexpressing VEGF,[24] and mice with mutations in the procollagen IV gene[28] (Table S1). Numerous mouse models have also identified neurovascular pathways regulating GM vessel maturation,[23–25,29,48] endothelial cell pathways which maintain GM vascular integrity,[26] pathways in pericytes which regulate vascular morphogenesis in the GM,[27] and genetic mutations that have important implications in GM-IVH.[28,49] While these studies have made valuable advances in our understanding of the cellular mechanisms mediating GM vascular stability, they often rely on knowledge acquired from select specific time points, and their conclusions are based on the data derived from human samples. Knowledge pertaining to the development of the mouse GM and a detailed study of GM vascularization is lacking, preventing the adequate assessment of the information derived from mouse models in the study of GM-IVH.

In this work, we report the developmental stages of GM growth and involution in mice to provide insight into

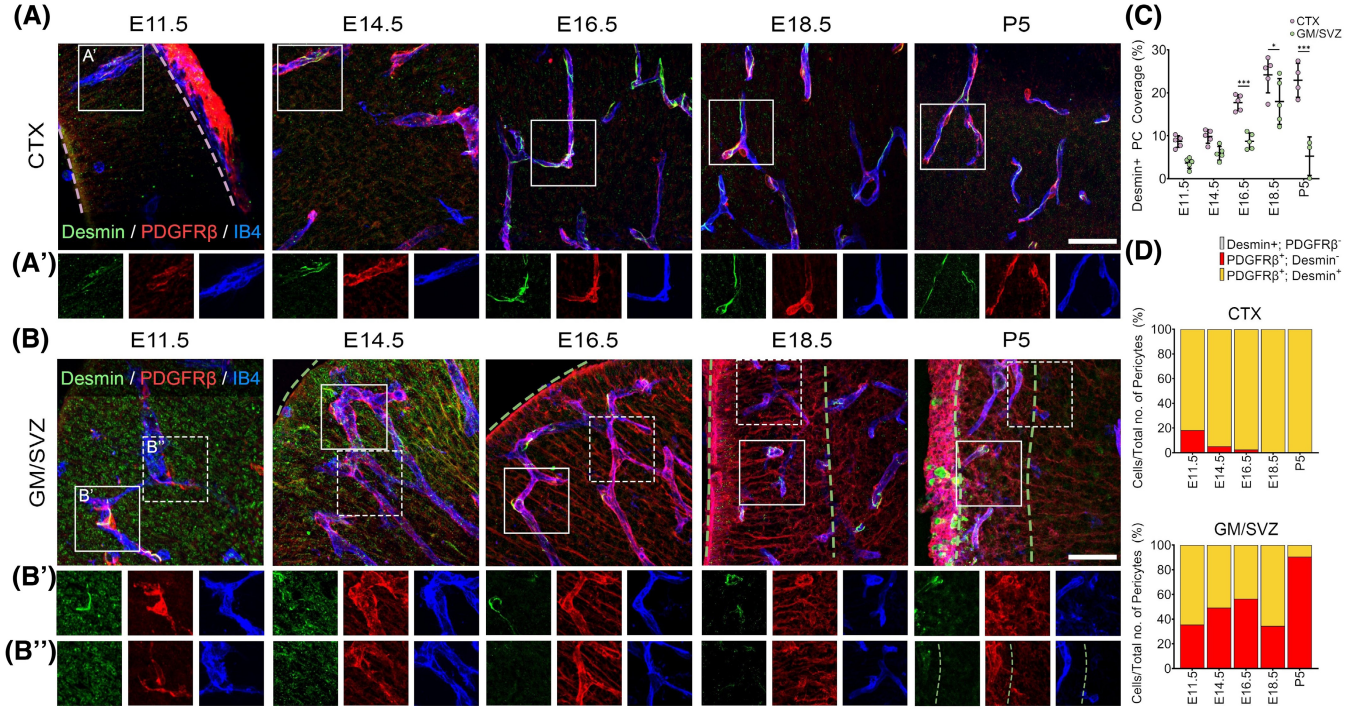

FIGURE 5 Desmin-positive pericyte coverage is deficient in the mouse GM. (A,B) High magnification images of the developing cortex (CTX) and the germinal matrix/postnatal subventricular zone (GM/SVZ) stained for blood vessels using Isolectin B4 (IB4, blue) and for pericytes with anti-PDGFRβ (red) and anti-Desmin (green).[63] Purple dashed lines mark the CTX, and green dashed lines highlight the GM/SVZ regions. Cropped individual images (white solid boxes) of the endothelium and pericytes are displayed below each timepoint to better visualize the overlap of Desmin and PDGFRβ expression (A′,B′). Additional cropped images (dashed white boxes) are displayed in B″ to visualize reduced Desmin-positive pericyte coverage of the GM blood vessels. (C) Quantification of Desmin-positive pericyte coverage reveals significantly reduced coverage at E16.5 and E18.5 in the GM and at P5 in the SVZ. Scatter dot plot shows mean values with standard deviation. $n = 5$ per time point except P5 ($n = 3$). Data was analyzed using a two-way ANOVA with Bonferroni's multiple comparison test. $^{**}p < .01$, $^{***}p < .001$. (D) Quantification of Desmin$^+$; PDGFRβ$^-$ (gray), PDGFRβ$^+$; Desmin$^-$ (red) and PDGFRβ$^+$; Desmin$^+$ (yellow) pericytes over total pericytes counted per field. $n = 5$ per time point except P5 ($n = 3$). LV, lateral ventricles; E, embryonic; P, postnatal. Scale bar, 50 μm

the mouse GM dynamics. Specifically, we found that the GM begins growing in size at E10.5 and reaches its widest size at E14.5. Interestingly, previous descriptions of neural progenitor cell (NPC) proliferation in mice greatly overlaps with the stages of GM growth we have identified. NPC proliferation in mice is documented to begin at E10.5, with the appearance of the medial ganglionic eminence and peak at E14/E15 after which proliferation declines.[39,50,51] This is analogous to the dynamics of the GM in humans where GM expansion also corresponds with NPC proliferation.[3]

Our results also show that the mouse GM vasculature has greater vessel area and number of vessel branches compared to the cerebral CTX at most of the time points analyzed. This finding of higher vascularity in the mouse GM is comparable to the observations from the human GM which also report a greater vessel area and number of blood vessels.[9] The increased vessel area and vessel branches, but not vessel diameter in both the mouse and human GM compared to other areas of the developing brain point to a greater angiogenic response of the GM. This supports the current concept that the vasculature of the GM is immature compared to other regions of the brain, which may explain the susceptibility of the GM vasculature to hemorrhage.

Evaluation of PDGFRβ-positive pericyte coverage between the GM and the cerebral CTX in mice reveals similar pericyte coverage between the two brain regions during embryonic development. Other studies in mice present similar results in which pericyte coverage in the embryonic brain vasculature was comparable across different brain regions.[25] However, this finding is in contrast to the reports on the developing human brain where there is a paucity in pericyte coverage in the GM.[13] The subjects used in human studies are variable and consist of premature infants of 23–40 weeks of gestation age and abortuses of 16–22 weeks[13]; it is likely that factors such as the mode of delivery and the clinical status of human subjects in addition to the molecular[52] and functional[53] differences between the mouse, and

human brain vasculatures contribute to the discrepancies observed.

Assessment of other pericyte markers in the GM shows significantly lower NG2-positive pericyte coverage in the GM at E11.5 compared to the CTX. Consistent with this, we observe more PDGFRβ$^+$; NG2$^-$ pericytes in the GM at E11.5 than in the CTX. NG2 has been previously reported as a marker for pericytes expressed later than PDGFRβ[35,41]; hence, the differences observed in PDGFRβ and NG2 expression suggest that pericytes of the GM may be more immature during these early stages of angiogenesis. Similar heterogenous marker expression, PDGFRβ-positive and NG2-negative immunoreactivity patterns were observed in the cerebral CTX,[35] which we did not observe in our study. It is possible that if the PDGFRβ$^+$; NG2$^-$ population is, as suspected, a more immature precursor to the PDGFRβ$^+$; NG2$^+$ population with a short timeframe of existence, we might have missed in the timeline of our evaluation of CTX. In the human, PDGFRβ and NG2 expression in the early angiogenic GM has not been reported prior to 17 weeks of gestational age[13]; it is, therefore, difficult to derive similarities or differences in early pericyte differentiation and expression of PDGFRβ and NG2 between the mouse and human GM.

Additional investigation into the mouse GM pericytes using Desmin shows pericytes of the GM are distinct from those of the developing cerebral CTX. In the GM, the expression and distribution of PDGFRβ$^+$; Desmin$^+$ pericytes is highly variable when compared to the CTX. Desmin is an intermediate filament protein that is required for contractile functions.[42] It is expressed by both mature and immature pericytes, and its expression is suggested to be a measure of vessel stability.[35,54] The lack of Desmin expression in the GM pericytes may contribute to the fragility of the GM vessels. However to date, it is unknown what Desmin-positive pericyte coverage is in the human GM as the only information reported is that very few pericytes of the developing human brain express Desmin.[13] To the best of our knowledge any additional differences in pericyte marker expression in human samples and animal models of GM-IVH have yet to be described.

A question that remains unresolved and opens an exciting follow-up of this work relates to the molecular factors in pericytes which differ between the GM and other brain regions. Several ligand-receptor signaling pathways are known to mediate pericyte and endothelial interactions.[14] Ballabh et al evaluated the differential expression of several ligand-receptor pathways essential for pericyte recruitment and maturation in the healthy developing human fetal GM.[13] The pathways evaluated include angiopoietin, platelet-derived growth factor-B (PDGF-B), transforming growth factor-beta 1 (TGF-β1), sphingosine-1-phosphate (S1P) and their respective receptors. Their work describes lower expression of TGF-β protein and higher expressions of S1P1 and neural cadherin (N-cadherin) levels in the fetal GM than the CTX. In mice, pericyte-specific deletion of the TGF-β protein receptor Alk5 leads to GM-IVH, underpinning the importance of pericytes in stabilizing the GM vasculature in mice[27] while also underscoring the molecular similarities between the mouse and human GM pericytes. These studies provide some insight into the possible molecular cues regulating the pericyte heterogeneity described in our study and support the concept that despite the similarities in pericyte coverage between the mouse GM and the CTX, mouse GM pericytes are phenotypically and functionally heterogenous. Future studies exploring pericyte heterogeneity and the mechanistic regulation of pericyte function between the GM and other regions of the brain will further contribute to the overall understanding of pericyte biology and will also provide insight into the phenotypical and functional differences of GM pericytes which influence the susceptibility of the GM vasculature to hemorrhage.

Brain pericytes are uniquely positioned within the neurovascular unit (NVU) to interact with other cell types, such as neurons and astrocytes, which are also present within the NVU. In the mature mouse brain, pericytes are able to communicate and regulate neuronal survival by the release of neurotrophic factors or through communication with astrocytes.[22,55] Very little, however, is known about how pericytes might interact with NPCs in the GM. Interestingly, similar to pericyte coverage, glial fibrillary acidic protein (GFAP) expression in astrocyte end-feet of the healthy fetal GM is deficient compared to CTX.[56] This decrease in GFAP expression is speculated to also contribute to the fragility of the GM vasculature and its propensity to hemorrhage. Different mouse models have demonstrated the importance of pericyte-astrocyte communication in the regulation of blood-brain barrier stability,[17,57,58] which is further supported by in vitro data reporting that astrocytes modulate pericyte synthesis of extracellular matrix molecules essential for providing structural stability to the vasculature.[59] However, it has yet to be reported whether pericytes are in close interaction with astrocytes during development of the healthy fetal GM. A comprehensive evaluation of pericyte interaction and communication with other cell types during the development of the GM and in animal models of GM-IVH (Table S1) would be of great value to further our understanding of GM-IVH pathogenesis.

GM-IVH-induced neuroinflammation is one of the most relevant pathological features associated with brain injury to the white matter that may contribute to long-term neurological complications.[60] Many of the animal models of GM-IVH are associated with an inflammatory response such as increased neutrophil infiltration, activated microglia and

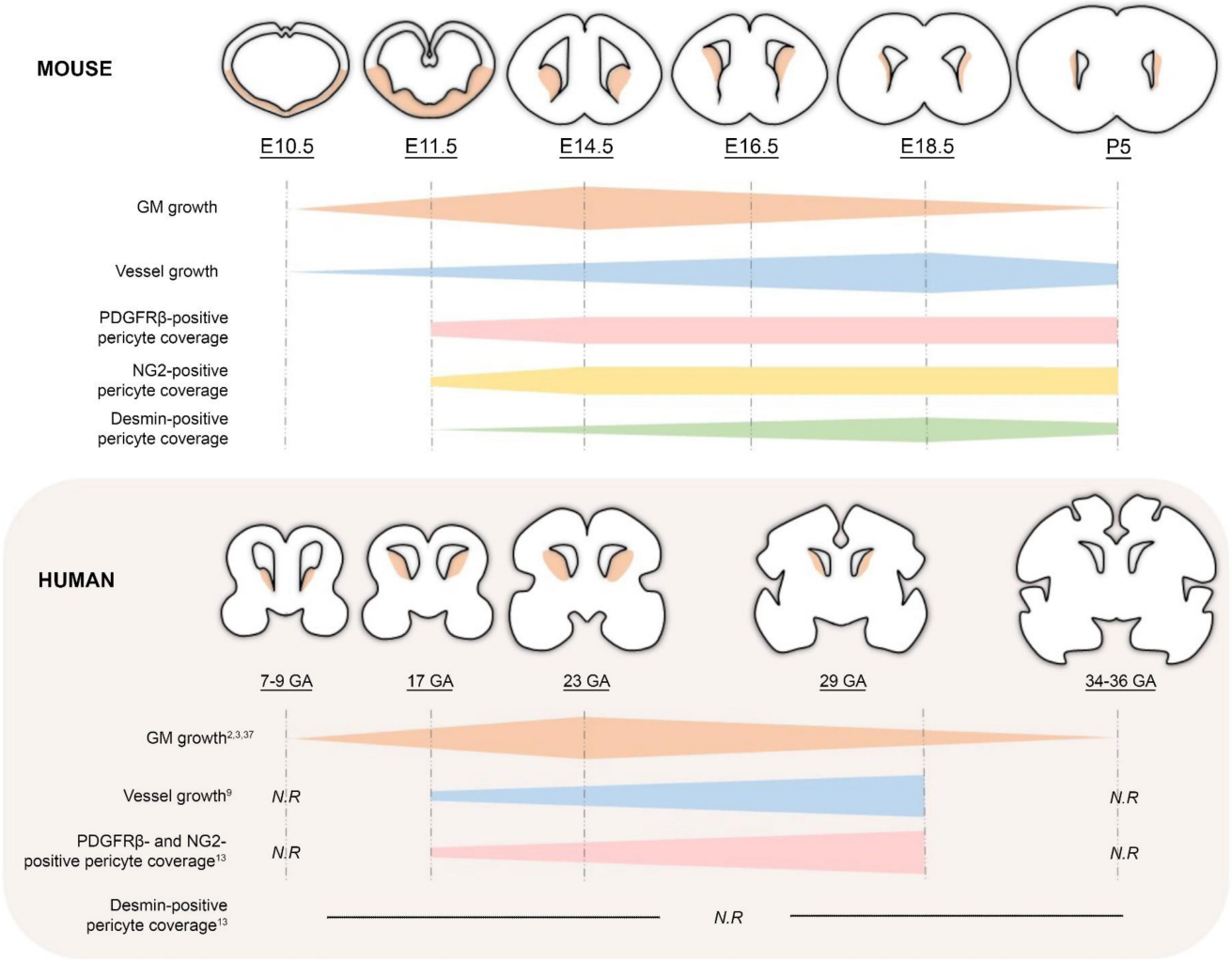

FIGURE 6 Comparison of the mouse and human GM growth, angiogenesis and pericyte coverage during development. Note that data on the human vessel growth and pericyte coverage is not reported (N.R.) for early (<17 GA) and late gestational ages (>34 GA). E, embryonic; P, postnatal; GA, gestational age (weeks)

gliosis.[61] Interestingly, pericytes have been reported to regulate immune responses in the central nervous system.[16,62] However, whether the differences in pericytes between the GM and other brain regions is a contributing factor to the progression of neuroinflammation in GM-IVH, and how neuroinflammation might affect the expression of pericyte markers, pericyte coverage, and pericyte morphology in GM-IVH remains to be established.

Today, the most effective strategy for the prevention of GM-IVH is to reduce the risk of GM-IVH using prenatal and postnatal interventions. The most common treatment is the administration of antenatal glucocorticoids, which are used to prevent respiratory distress syndrome in premature infants.[8] Understanding the pathogenesis of GM-IVH is necessary for a more specific and targeted therapeutic intervention. Through this study, we have provided a comprehensive examination of the mouse GM and compared it to the previously reported findings on the human GM, as summarized in Figure 6. We have identified key similarities and differences between the mouse and human GM; while not all aspects of the mouse GM model that of the human, the mouse remains, nonetheless, useful for genetic manipulations or experimental inductions which are key to further our much needed understanding of GM-IVH pathogenesis.

ACKNOWLEDGEMENTS

We would like to thank Jan Kitajewski, Daniel Shaye, Naiche Adler, and Sarah Lutz for helpful discussions. Also, we appreciate all the feedback received on this project from the Cuervo, Kitajewski, Shaye and Lutz laboratory members. We also thank the laboratory support provided by Prasanth Punathil from the Cuervo laboratory. This work was supported by start-up funds from the University of Illinois Chicago to HC and the UIC Provost's Award for Graduate Research (TN).

DISCLOSURES

The author(s) have declared no potential conflicts of interests with respect to the research, authorship, and/or publication of this article.

AUTHOR CONTRIBUTIONS

TN and HC designed the studies, conducted experiments, acquired data, analyzed the data, and wrote the manuscript. AB conducted experiments and LB analyzed the data.

DATA AVAILABILITY STATEMENT

The authors confirm that the data supporting the findings of this study are available within the article and its supplementary materials.

ORCID

Henar Cuervo https://orcid.org/0000-0001-8293-9377

REFERENCES

1. Ballabh P. Pathogenesis and prevention of intraventricular hemorrhage. *Clin Perinatol*. 2014;41(1):47-67.
2. Kinoshita Y, Okudera T, Tsuru E, Yokota A. Volumetric analysis of the germinal matrix and lateral ventricles performed using MR images of postmortem fetuses. *AJNR Am J Neuroradiol*. 2001;22(2):382-388.
3. Del Bigio MR. Cell proliferation in human ganglionic eminence and suppression after prematurity-associated haemorrhage. *Brain*. 2011;134(Pt 5):1344-1361.
4. Ancel P-Y, Livinec F, Larroque B, et al. Cerebral palsy among very preterm children in relation to gestational age and neonatal ultrasound abnormalities: the EPIPAGE cohort study. *Pediatrics*. 2006;117(3):828-835.
5. Patra K, Wilson-Costello D, Taylor HG, Mercuri-Minich N, Hack M. Grades I-II intraventricular hemorrhage in extremely low birth weight infants: effects on neurodevelopment. *J Pediatr*. 2006;149(2):169-173.
6. Vavasseur C, Slevin M, Donoghue V, Murphy JF. Effect of low grade intraventricular hemorrhage on developmental outcome of preterm infants. *J Pediatr*. 2007;151(2):e6; author reply e6–7. 10.1016/j.jpeds.2007.03.051
7. Klebermass-Schrehof K, Czaba C, Olischar M, et al. Impact of low-grade intraventricular hemorrhage on long-term neurodevelopmental outcome in preterm infants. *Childs Nerv Syst*. 2012;28(12):2085-2092.
8. Lekic T, Klebe D, Pichon P, et al. Aligning animal models of clinical germinal matrix hemorrhage, from basic correlation to therapeutic approach. *Curr Drug Targets*. 2017;18(12):1316-1328.
9. Ballabh P, Braun A, Nedergaard M. Anatomic analysis of blood vessels in germinal matrix, cerebral cortex, and white matter in developing infants. *Pediatr Res*. 2004;56(1):117-124.
10. Inder TE, Perlman JM, Volpe JJ, et al. Chapter 24 – Preterm intraventricular hemorrhage/posthemorrhagic hydrocephalus. In: Volpe JJ, Inder TE, Darras BT, eds. *Volpe's neurology of the newborn* (6th ed.). Elsevier; 2018:637-698.e21.
11. Ballabh P, Xu H, Hu F, et al. Angiogenic inhibition reduces germinal matrix hemorrhage. *Nat Med*. 2007;13(4):477-485.
12. Ferrara N, Gerber HP, LeCouter J. The biology of VEGF and its receptors. *Nat Med*. 2003;9(6):669-676.
13. Braun A, Xu H, Hu F, et al. Paucity of pericytes in germinal matrix vasculature of premature infants. *J Neurosci*. 2007;27(44):12012-12024.
14. Armulik A, Genove G, Betsholtz C. Pericytes: developmental, physiological, and pathological perspectives, problems, and promises. *Dev Cell*. 2011;21(2):193-215.
15. Winkler EA, Bell RD, Zlokovic BV. Central nervous system pericytes in health and disease. *Nat Neurosci*. 2011;14(11):1398-1405.
16. Daneman R, Zhou L, Kebede AA, Barres BA. Pericytes are required for blood-brain barrier integrity during embryogenesis. *Nature*. 2010;468(7323):562-566.
17. Armulik A, Genové G, Mäe M, et al. Pericytes regulate the blood-brain barrier. *Nature*. 2010;468(7323):557-561.
18. Lindblom P, Gerhardt H, Liebner S, et al. Endothelial PDGF-B retention is required for proper investment of pericytes in the microvessel wall. *Genes Dev*. 2003;17(15):1835-1840.
19. Lindahl P, Johansson BR, Leveen P, Betsholtz C. Pericyte loss and microaneurysm formation in PDGF-B-deficient mice. *Science*. 1997;277(5323):242-245.
20. Eilken HM, Diéguez-Hurtado R, Schmidt I, et al. Pericytes regulate VEGF-induced endothelial sprouting through VEGFR1. *Nat Commun*. 2017;8(1):1574.
21. Stratman AN, Malotte KM, Mahan RD, Davis MJ, Davis GE. Pericyte recruitment during vasculogenic tube assembly stimulates endothelial basement membrane matrix formation. *Blood*. 2009;114(24):5091-5101.
22. Sweeney MD, Ayyadurai S, Zlokovic BV. Pericytes of the neurovascular unit: key functions and signaling pathways. *Nat Neurosci*. 2016;19(6):771-783.
23. Ma S, Santhosh D, Kumar TP, Huang Z. A brain-region-specific neural pathway regulating germinal matrix angiogenesis. *Dev Cell*. 2017;41(4):366-381.e4.
24. Yang D, Baumann JM, Sun Y-Y, et al. Overexpression of vascular endothelial growth factor in the germinal matrix induces neurovascular proteases and intraventricular hemorrhage. *Sci Transl Med*. 2013;5(193):ra90. 10.1126/scitranslmed.3005794
25. Licht T, Dor-Wollman T, Ben-Zvi A, Rothe G, Keshet E. Vessel maturation schedule determines vulnerability to neuronal injuries of prematurity. *J Clin Invest*. 2015;125(3):1319-1328.
26. Li F, Lan YU, Wang Y, et al. Endothelial Smad4 maintains cerebrovascular integrity by activating N-cadherin through cooperation with Notch. *Dev Cell*. 2011;20(3):291-302.
27. Dave JM, Mirabella T, Weatherbee SD, Greif DM. Pericyte ALK5/TIMP3 axis contributes to endothelial morphogenesis in the developing brain. *Dev Cell*. 2018;47(3):388-389.
28. Gould DB, Phalan FC, Breedveld GJ, et al. Mutations in Col4a1 cause perinatal cerebral hemorrhage and porencephaly. *Science*. 2005;308(5725):1167-1171.
29. Arnold TD, Niaudet C, Pang MF, et al. Excessive vascular sprouting underlies cerebral hemorrhage in mice lacking alphaVbeta8-TGFbeta signaling in the brain. *Development*. 2014;141(23):4489-4499.
30. Cuervo H, Pereira B, Nadeem T, et al. PDGFRbeta-P2A-CreER(T2) mice: a genetic tool to target pericytes in angiogenesis. *Angiogenesis*. 2017;20(4):655-662.
31. Madisen L, Zwingman TA, Sunkin SM, et al. A robust and high-throughput Cre reporting and characterization system for the whole mouse brain. *Nat Neurosci*. 2010;13(1):133-140.

32. Muzumdar MD, Tasic B, Miyamichi K, Li L, Luo L. A global double-fluorescent Cre reporter mouse. *Genesis*. 2007;45(9):593-605.
33. Guide for the Care and Use of Laboratory Animals. *The National Academies Collection: reports funded by National Institutes of Health*. The National Academies Press; 2011.
34. Abramsson A, Lindblom P, Betsholtz C. Endothelial and non-endothelial sources of PDGF-B regulate pericyte recruitment and influence vascular pattern formation in tumors. *J Clin Invest*. 2003;112(8):1142-1151.
35. Jung B, Arnold TD, Raschperger E, Gaengel K, Betsholtz C. Visualization of vascular mural cells in developing brain using genetically labeled transgenic reporter mice. *J Cereb Blood Flow Metab*. 2018;38(3):456-468.
36. Volpe JJ. Brain injury in premature infants: a complex amalgam of destructive and developmental disturbances. *Lancet Neurol*. 2009;8(1):110-124.
37. Letinic K, Kostovic I. Transient fetal structure, the gangliothalamic body, connects telencephalic germinal zone with all thalamic regions in the developing human brain. *J Comp Neurol*. 1997;384(3):373-395.
38. Chen VS, Morrison JP, Southwell MF, Foley JF, Bolon B, Elmore SA. Histology atlas of the developing prenatal and postnatal mouse central nervous system, with emphasis on prenatal days E7.5 to E18.5. *Toxicol Pathol*. 2017;45(6):705-744.
39. Brazel CY, Romanko MJ, Rothstein RP, Levison SW. Roles of the mammalian subventricular zone in brain development. *Prog Neurogibol*. 2003;69(1):49-69.
40. Vasudevan A, Long JE, Crandall JE, Rubenstein JL, Bhide PG. Compartment-specific transcription factors orchestrate angiogenesis gradients in the embryonic brain. *Nat Neurosci*. 2008;11(4):429-439.
41. Yamanishi E, Takahashi M, Saga Y, Osumi N. Penetration and differentiation of cephalic neural crest-derived cells in the developing mouse telencephalon. *Dev Growth Differ*. 2012;54(9):785-800.
42. Paulin D, Li Z. Desmin: a major intermediate filament protein essential for the structural integrity and function of muscle. *Exp Cell Res*. 2004;301(1):1-7.
43. Tang DD. Intermediate filaments in smooth muscle. *Am J Physiol Cell Physiol*. 2008;294(4):C869-C878.
44. Georgiadis P, Xu H, Chua C, et al. Characterization of acute brain injuries and neurobehavioral profiles in a rabbit model of germinal matrix hemorrhage. *Stroke*. 2008;39(12):3378-3388.
45. Dawes WJ, Zhang X, Fancy SPJ, Rowitch D, Marino S. Moderate-grade germinal matrix haemorrhage activates cell division in the neonatal mouse subventricular zone. *Dev Neurosci*. 2016;38(6):430-444.
46. Krafft PR, Rolland WB, Duris K, et al. Modeling intracerebral hemorrhage in mice: injection of autologous blood or bacterial collagenase. *J Vis Exp*. 2012;67:e4289.
47. McCarty JH, Monahan-Earley RA, Brown LF, et al. Defective associations between blood vessels and brain parenchyma lead to cerebral hemorrhage in mice lacking alphav integrins. *Mol Cell Biol*. 2002;22(21):7667-7677.
48. Proctor JM, Zang K, Wang D, Wang R, Reichardt LF. Vascular development of the brain requires beta8 integrin expression in the neuroepithelium. *J Neurosci*. 2005;25(43):9940-9948.
49. Bilguvar K, DiLuna ML, Bizzarro MJ, et al. COL4A1 mutation in preterm intraventricular hemorrhage. *J Pediatr*. 2009;155(5):743-745.
50. Smart IH. A pilot study of cell production by the ganglionic eminences of the developing mouse brain. *J Anat*. 1976;121(Pt 1):71-84.
51. Turrero Garcia M, Harwell CC. Radial glia in the ventral telencephalon. *FEBS Lett*. 2017;591(24):3942-3959.
52. Song HW, Foreman KL, Gastfriend BD, Kuo JS, Palecek SP, Shusta EV. Transcriptomic comparison of human and mouse brain microvessels. *Sci Rep*. 2020;10(1):12358.
53. O'Brown NM, Pfau SJ, Gu C. Bridging barriers: a comparative look at the blood-brain barrier across organisms. *Genes Dev*. 2018;32(7-8):466-478.
54. Hellstrom M, Kalen M, Lindahl P, Abramsson A, Betsholtz C. Role of PDGF-B and PDGFR-beta in recruitment of vascular smooth muscle cells and pericytes during embryonic blood vessel formation in the mouse. *Development*. 1999;126(14):3047-3055.
55. Geranmayeh MH, Rahbarghazi R, Farhoudi M. Targeting pericytes for neurovascular regeneration. *Cell Commun Signal*. 2019;17(1):26.
56. El-Khoury N, Braun A, Hu F, et al. Astrocyte end-feet in germinal matrix, cerebral cortex, and white matter in developing infants. *Pediatr Res*. 2006;59(5):673-679.
57. Bonkowski D, Katyshev V, Balabanov RD, Borisov A, Dore-Duffy P. The CNS microvascular pericyte: pericyte-astrocyte crosstalk in the regulation of tissue survival. *Fluids Barriers CNS*. 2011;8(1):8.
58. Gundersen GA, Vindedal GF, Skare O, Nagelhus EA. Evidence that pericytes regulate aquaporin-4 polarization in mouse cortical astrocytes. *Brain Struct Funct*. 2014;219(6):2181-2186.
59. Jiang B, Liou GI, Behzadian MA, Caldwell RB. Astrocytes modulate retinal vasculogenesis: effects on fibronectin expression. *J Cell Sci*. 1994;107(Pt 9):2499-2508.
60. Ballabh P, de Vries LS. White matter injury in infants with intraventricular haemorrhage: mechanisms and therapies. *Nat Rev Neurol*. 2021;17(4):199-214.
61. Atienza-Navarro I, Alves-Martinez P, Lubian-Lopez S, Garcia-Alloza M. Germinal matrix-intraventricular hemorrhage of the preterm newborn and preclinical models: inflammatory considerations. *Int J Mol Sci*. 2020;21(21):8343.
62. Török O, Schreiner B, Schaffenrath J, et al. Pericytes regulate vascular immune homeostasis in the CNS. *Proc Natl Acad Sci USA*. 2021;118(10). 10.1073/pnas.2016587118
63. Couto JA, Huang AY, Konczyk DJ, et al. Somatic MAP2K1 mutations are associated with extracranial arteriovenous malformation. *Am J Hum Genet*. 2017;100(3):546-554.
64. Chua CO, Chahboune H, Braun A, et al. Consequences of intraventricular hemorrhage in a rabbit pup model. *Stroke*. 2009;40(10):3369-3377.
65. Vinukonda G, Dohare P, Arshad A, et al. Hyaluronidase and hyaluronan oligosaccharides promote neurological recovery after intraventricular hemorrhage. *J Neurosci*. 2016;36(3):872-889.
66. Vinukonda G, Csiszar A, Hu F, et al. Neuroprotection in a rabbit model of intraventricular haemorrhage by cyclooxygenase-2, prostanoid receptor-1 or tumour necrosis factor-alpha inhibition. *Brain*. 2010;133(Pt 8):2264-2280.
67. Cherian SS, Love S, Silver IA, Porter HJ, Whitelaw AG, Thoresen M. Posthemorrhagic ventricular dilation in the neonate: development and characterization of a rat model. *J Neuropathol Exp Neurol*. 2003;62(3):292-303.
68. Goulding DS, Vogel RC, Gensel JC, Morganti JM, Stromberg AJ, Miller BA. Acute brain inflammation, white matter oxidative

stress, and myelin deficiency in a model of neonatal intraventricular hemorrhage. *J Neurosurg Pediatr*. 2020;26(6):613-623.
69. Garton TP, He Y, Garton HJ, Keep RF, Xi G, Strahle JM. Hemoglobin-induced neuronal degeneration in the hippocampus after neonatal intraventricular hemorrhage. *Brain Res*. 2016;1635:86-94.
70. Lekic T, Manaenko A, Rolland W, et al. Rodent neonatal germinal matrix hemorrhage mimics the human brain injury, neurological consequences, and post-hemorrhagic hydrocephalus. *Exp Neurol*. 2012;236(1):69-78.
71. Klebe D, Krafft PR, Hoffmann C, et al. Acute and delayed deferoxamine treatment attenuates long-term sequelae after germinal matrix hemorrhage in neonatal rats. *Stroke*. 2014;45(8):2475-2479.
72. Segado-Arenas A, Infante-Garcia C, Benavente-Fernandez I, et al. Cognitive impairment and brain and peripheral alterations in a murine model of intraventricular hemorrhage in the preterm newborn. *Mol Neurobiol*. 2018;55(6):4896-4910.

SUPPORTING INFORMATION

Additional supporting information may be found in the online version of the article at the publisher's website.

How to cite this article: Nadeem T, Bommareddy A, Bolarinwa L, Cuervo H. Pericyte dynamics in the mouse germinal matrix angiogenesis. *FASEB J*. 2022;36:e22339. doi:10.1096/fj.202200120R